UC Berkeley
UC Berkeley Previously Published Works

Title

Controlling the Reduction of Chelated Uranyl to Stable Tetravalent Uranium Coordination Complexes in Aqueous Solution

Authors

Carter, Korey P
Smith, Kurt F
Tratnjek, Toni
et al.

Controlling the Reduction of Chelated Uranyl to Stable Tetravalent Uranium Coordination Complexes in Aqueous Solution

Korey P. Carter, Kurt F. Smith, Toni Tratnjek, Gauthier J.-P. Deblonde, Liane M. Moreau, Julian A. Rees, Corwin H. Booth,* and Rebecca J. Abergel*

Read Online

ACCESS | Metrics & More | Article Recommendations | Supporting Information

ABSTRACT: The solution-state interactions between octadentate hydroxypyridinone (HOPO) and catecholamide (CAM) chelating ligands and uranium were investigated and characterized by UV−visible spectrophotometry and X-ray absorption spectroscopy (XAS), as well as electrochemically via spectroelectrochemistry (SEC) and cyclic voltammetry (CV) measurements. Depending on the selected chelator, we demonstrate the controlled ability to bind and stabilize U^{IV}, generating with 3,4,3-LI(1,2-HOPO), a tetravalent uranium complex that is practically inert toward oxidation or hydrolysis in acidic, aqueous solution. At physiological pH values, we are also able to bind and stabilize U^{IV} to a lesser extent, as evidenced by the mix of U^{IV} and U^{VI} complexes observed via XAS. CV and SEC measurements confirmed that the U^{IV} complex formed with 3,4,3-LI(1,2-HOPO) is redox inert in acidic media, and U^{VI} ions can be reduced, likely proceeding via a two-electron reduction process.
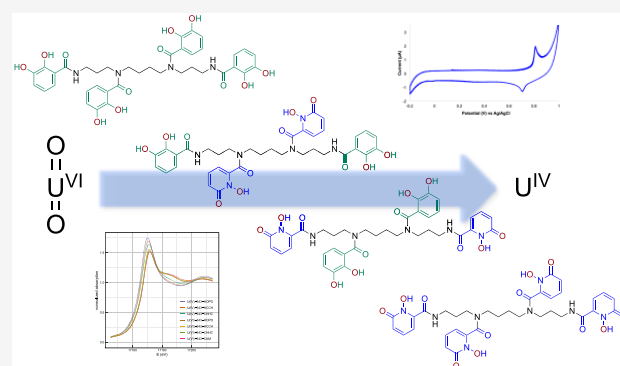

INTRODUCTION

As the use of actinides in both the nuclear power and defense sectors over the past 70 years has resulted in environmental releases of radionuclides generated during associated activities,[1−3] the development of aqueous actinide chelation chemistry remains continuously relevant.[4,5] Understanding the fundamental bonding interactions of individual actinide cations is critical for ongoing efforts focused on improving actinide decorporation therapies and developing new environmental remediation strategies. This is particularly true for the highly water-soluble uranyl cation, $U^{VI}O_2^{2+}$, which is the predominant form of uranium (U) found in the environment.[6,7] The significant mobility of the uranyl cation introduces risks for radiological contamination, which is a crucial public health issue, as uranium exhibits both chemical and radiological toxicity.[8] Once internalized in the human body, U ions move rapidly throughout the bloodstream and are primarily deposited in the kidney and the skeleton.[9,10] Clearance following uptake and deposition of U is known to be slow, with decorporation via metal-ion chelation considered the best method for promoting excretion of actinides *in vivo*. However, despite significant research efforts in this area, there are no effective chelators for U decorporation currently approved by the U.S. Food and Drug Administration, and the sole approved actinide decorporation ligand, diethylenetriaminepentaacetic acid (DTPA), is contraindicated for the treatment of U contamination, as it may favor the translocation of U and increase the metal concentration in specific biological compartments such as the kidneys.[11,12]

Multidentate hydroxypyridinone (HOPO) and catecholamide (CAM) ligands are known to chelate both actinide (An) and lanthanide (Ln) cations exceptionally well both *in vitro* and *in vivo*,[4,13,14] and have been shown to be effective decorporation agents of trivalent and tetravalent actinides in multiple animal models.[12,15,16] The octadentate 3,4,3-LI(1,2-HOPO) (Scheme 1), denoted 343-HOPO hereafter,[11] was designed for tetravalent plutonium (Pu) chelation,[4,11] and has proven exemplary for coordinating a range of tetravalent p-, d-, and f-block metals.[17−22] Moreover, it has been shown to significantly increase excretion *in vivo* of actinyl species such as U^{VI} and Np^{V},[12] although the mechanism for these latter findings is not well understood. The coordination chemistry and solution thermodynamics of $[UO_2]^{2+}$-343-HOPO binding have been investigated in several studies, revealing that 343-HOPO binding with hexavalent uranium is less thermodynamically favorable than that of other targets such as Pu^{IV}.[10,18,23] We recently observed 343-HOPO chelation-driven activation and concurrent reduction of the neptunyl(V) cation to
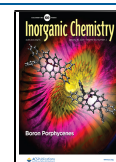
Scheme 1. Spermine-Based Octadentate Ligands[1]
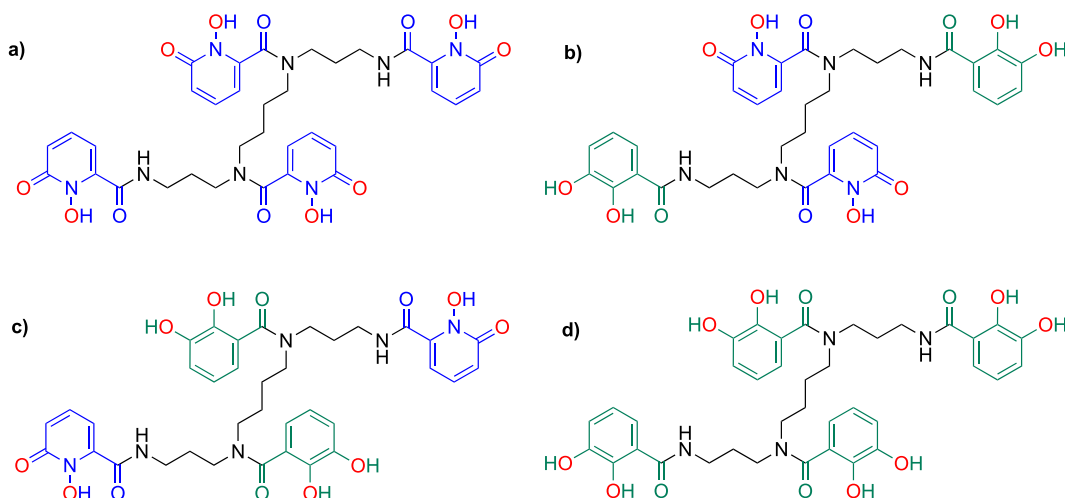
[1]For each ligand, the 3,4,3-LI scaffold is connected through amide linkages to four metal-binding units, which are either 1,2-HOPO (blue) or CAM (green) moieties (metal-binding atoms highlighted in red). Only four ligand combinations are easily accessible through classical synthetic methods: (a) 3,4,3-LI(1,2-HOPO), (b) 3,4,3-LI(CAM)$_2$(1,2-HOPO)$_2$, (c) 3,4,3-LI(1,2-HOPO)$_2$(CAM)$_2$, and (d) 3,4,3-LI(CAM) (respectively denoted 343-HOPO, 343-CHHC, 343-HCCH, and 343-CAM hereafter).
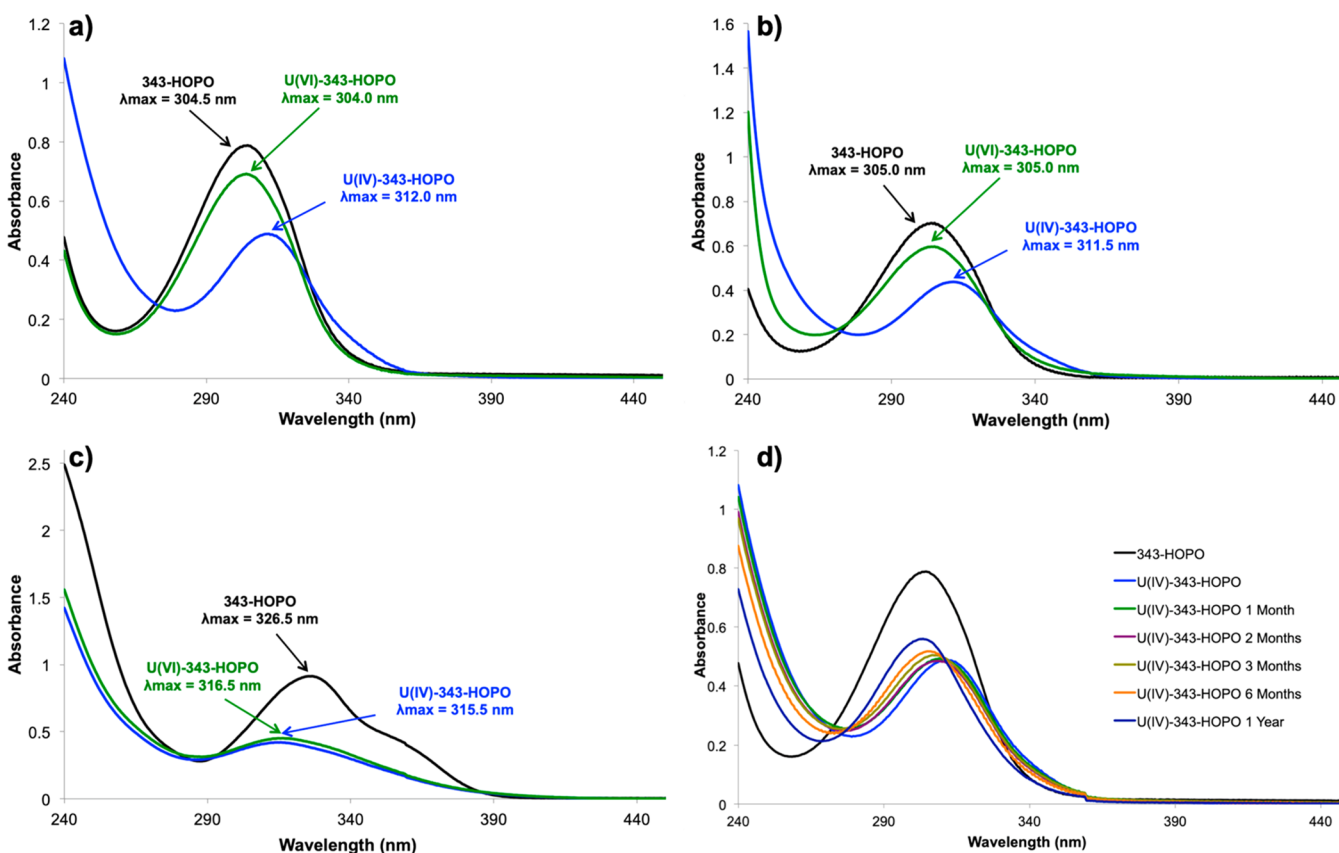

Figure 1. UV−vis absorbance spectra of samples containing: 25 μM of 343-HOPO (black curves), 25 μM of 343-HOPO and U^{IV} (blue curves), and 25 μM of 343-HOPO and U^{VI} (green curves). Background electrolyte: (a) 0.1 M HCl (pH 1), (b) 0.1 M H$_2$SO$_4$ (pH 1), (c) 20 mM HEPES (pH 7.4), and (d) 0.1 M HCl (pH 1). Path length: 1 cm. Absorbance corrected from blank background electrolyte for each sample. T = 25 °C.

Np^{IV},[22,24] and here we extended these efforts to investigate whether a similar chelation-induced reduction mechanism could occur in uranium systems.

The chemically-mediated reduction of U, from +VI to +IV, is known in synthetic schemes,[25−27] biological systems,[28] and the environment,[29] yet the reduction is complicated by the known instability of U^{IV} in the presence of molecular oxygen.[27,30] This complication makes the U^{VI}/U^{IV} redox couple hard to evaluate and has thus far limited the applicability of chelation-driven reduction as a means for U decorporation, although recent efforts have elucidated some details about U two-electron processes in both aqueous and

nonaqueous systems.[27,31−33] Here we began our investigation into uranium chelation by looking at fundamental binding interactions of U^{IV} and U^{VI} complexes featuring 343-HOPO as well as three synthetic analogs via UV−vis spectrophotometry. The additional 343 ligands are also built on the spermine backbone and incorporate either four CAM metal-binding groups, 3,4,3-LI(CAM) (Scheme 1), denoted 343-CAM hereafter,[34] or a combination of 1,2-HOPO and CAM moieties directed by selective attachment to the primary or secondary amines of the scaffold, 3,4,3-LI(CAM)$_2$(1,2-HOPO)$_2$ and 3,4,3-LI(1,2-HOPO)$_2$(CAM)$_2$, respectively abbreviated 343-CHHC and 343-HCCH (Scheme 1).[14] Detailed solution-state electronic and structural information for both U^{IV} and U^{VI} complexes were obtained via X-ray absorption near edge structure (XANES) and extended X-ray absorption fine structure (EXAFS) spectroscopies, which highlighted the capability of the 343-chelators, except 343-CAM, to stabilize U^{IV} complexes in aqueous media at physiologically relevant pH. Moreover, using spectroelectrochemistry (SEC) as well as cyclic voltammetry (CV) measurements, we were able to delineate mechanistic information related to U redox processes using 343-HOPO. These results are particularly notable as tetravalent actinides are prone to hydrolysis, even under very acidic conditions,[35] thus electrochemical characterization of aqueous U^{IV} complexes with organic ligands is scarce, with only a few known examples studied in aqueous systems.[30,36]

RESULTS AND DISCUSSION

Optical Absorption Spectroscopy. The UV−visible (UV−vis) absorbance spectra of 343-HOPO under acidic and neutral pH conditions upon addition of U^{IV} or U^{VI} are shown in Figure 1. The 1,2-HOPO chromophores are known to absorb light in the UV region, and in the case of 343-HOPO, there is a $\pi-\pi^*$ band centered at approximately 305 nm that, when fully protonated, is sensitive to metal binding, which manifests as changes in both extinction coefficient and wavelength of maximum absorbance. Compared to free 343-HOPO, the UV−vis spectrum is red-shifted upon addition of U^{IV} in 0.1 M HCl and 0.1 M H_2SO_4 by 7.5 and 6.5 nm, respectively, while the addition of U^{VI} in acidic media does not result in a peak shift and only yields small ($\sim$4000−6000 M^{-1} cm^{-1}) changes in extinction coefficients (Figure 1a,b). Taken together, these results indicate that U^{IV} is complexed by 343-HOPO, consistent with 343-HOPO binding behavior previously observed with tetravalent transition metals and f-elements,[17−21] while U^{VI} ions are largely free in 0.1 M HCl and 0.1 M H_2SO_4. In contrast, the UV−vis spectra recorded at pH 7.4 are blue-shifted by approximately 10 nm upon addition of U^{IV} and U^{VI}, compared to free 343-HOPO (Figure 1c). UV−vis spectra of the free chelators 343-CHHC, 343-HCCH, and 343-CAM, as well as corresponding spectra upon addition of U^{IV} or U^{VI}, at pH 7.4 are shown in Figure S1 (Supporting Information). In acidic media, each of these ligands is partially protonated due to the additional protons of the CAM functional groups,[14,34] and thus, no binding was observed with either U^{IV} or U^{VI}. Compared to the free chelators at pH 7.4, we note similar behavior to what was observed for 343-HOPO, as the UV−vis spectra upon addition of U^{IV} and U^{VI} are blue-shifted for each of the corresponding free 343-ligands (Figure S1, Supporting Information).

Inspired by the greater stability to oxidation of U^{IV} in acidic media,[37,38] we also investigated the long-term behavior of U^{IV}-343-HOPO complexes in acidic media and observed that in 0.1

M HCl, U^{IV}-343-HOPO is practically inert to oxidation as prolonged (1 year) exposure to air caused only slight changes in the UV−vis spectrum (Figure 1d). Experimental confirmation of inert U^{IV} complexes toward oxidation or hydrolysis in aqueous solutions is unusual, with only a few known examples.[27,30,39,40] Extended aging of U^{IV} in aqueous media can also lead to changes in metal-ion speciation;[35,40] however, this was not observed here via UV−vis or investigated via other techniques, which suggests the U^{IV}-343-HOPO complex is very stable, a likely result of the thermodynamic benefits of the chelate effect and the known selectivity of 343-HOPO for tetravalent metal cations.[41] To improve our understanding of U^{IV} and U^{VI} coordination by the 343-ligands, we turned to X-ray absorption spectroscopy.

X-ray Absorption Spectroscopy. XANES and EXAFS spectra were collected at the U L$_{III}$ absorption edge (see Supporting Information for details) on a series of aqueous samples featuring either U^{IV} or U^{VI} with each of the 343-ligands, which were all prepared at pH 7−8 to ensure ligand deprotonation and formation of a single species in solution. XANES and EXAFS spectroscopies are of particular interest for systems with accessible redox couples, such as those described herein, as they can be used to determine metal oxidation states in solution by comparing spectral features, edge energies, and local structure environments to known standards for a given element. XANES spectra at the U L$_{III}$-edge of all U^{IV}- and U^{VI}-343 ligand complexes, with the exception of U^{IV}-343-CAM, which precipitated prior to measurement, are shown in Figure 2. While edge energy shifts and white line positions are largely similar for U^{IV} and U^{VI} complexes (typically only $\sim$1 eV higher for U^{VI}),[42] spectra from U^{VI} actinyl systems have two characteristic features: (1) a general reduction in the amplitude of the white line and (2) a shoulder at approximately 17185 eV above the main white line peak at $\sim$17173 eV. This high energy feature in the XANES
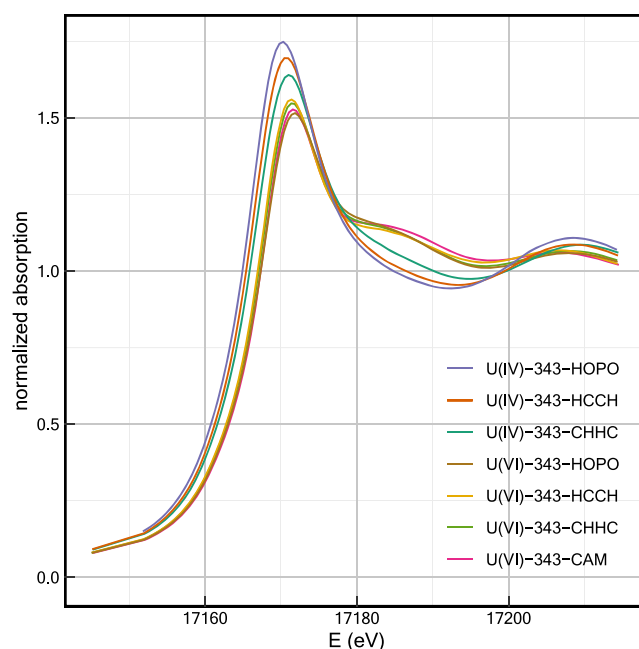
Figure 2. Comparison of U L$_{III}$-edge XANES spectra for aqueous U^{IV}- and U^{VI}-343 ligand complexes at 50 K. The presence of an "yl" shoulder at approximately 17185 eV in the U^{IV}-343-ligand spectra suggests a heterogeneous mixed U^{IV}/U^{VI} valence state.
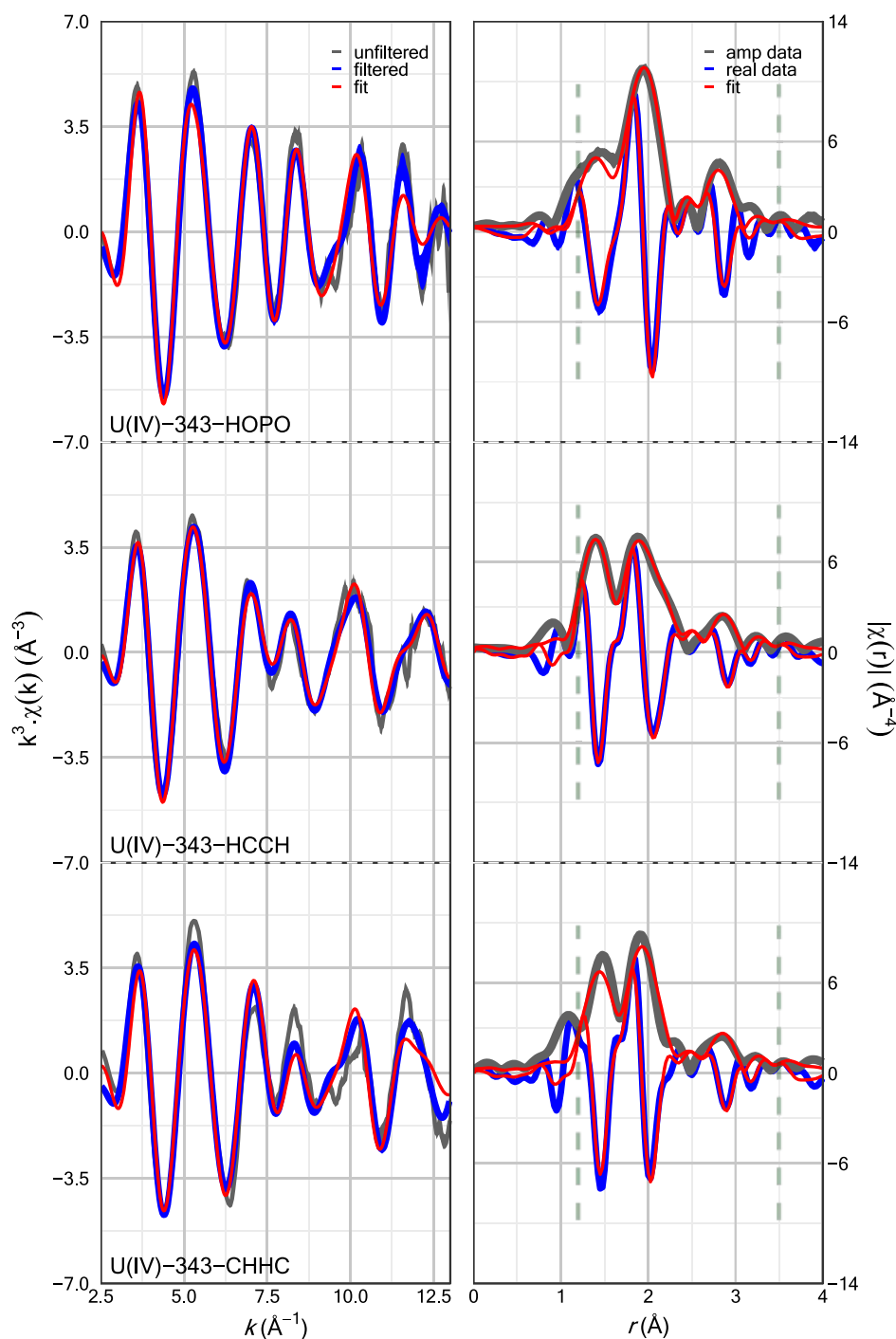
Figure 3. EXAFS data and fit results for aqueous U^{IV}-343 ligand complexes at 50 K. Left: EXAFS results in k-space. The filtered data and fit were back-transformed over the fit range (see the Supporting Information for details). Right: Fourier transforms (FT) of the k-space data and fit. Vertical dashed lines indicate the fit range. Data were transformed between 2.5 and 13.8 $Å^{-1}$ by using a 0.3 $Å^{-1}$ wide Gaussian window. The raw unfiltered data error bars (encompassed by the solid gray shaded area around the data set) were estimated by the standard deviation of the mean between traces.

spectra of U^{VI} complexes can be attributed to scattering associated with the axial oxygen atoms of the linear uranyl moiety and is often described as an "yl" shoulder. Both the reduced white line amplitude and "yl" shoulder features exist in the spectra of U^{IV}-343-HOPO, U^{IV}-343-HCCH, and U^{IV}-343-CHHC, albeit to a lower degree than in a pure U^{VI} system, hinting at possible heterogeneous mixed U^{IV}/U^{VI} valence state for each complex.

Compared with the growing collection of U^{IV} solid-state structures,[40,43−46] limited structural information is available for U^{IV} species in solution.[47−50] EXAFS spectroscopy was employed to acquire information about the local structure around U^{IV} cations, and high quality data were obtained from a wave vector, k, of 2.5 to a maximum of 13.8 $Å^{-1}$. Figure 3 shows the k^3-weighted U L_{III}-edge EXAFS spectra and corresponding Fourier transforms (FTs) with all fitting parameters included in Table S1 (Supporting Information).
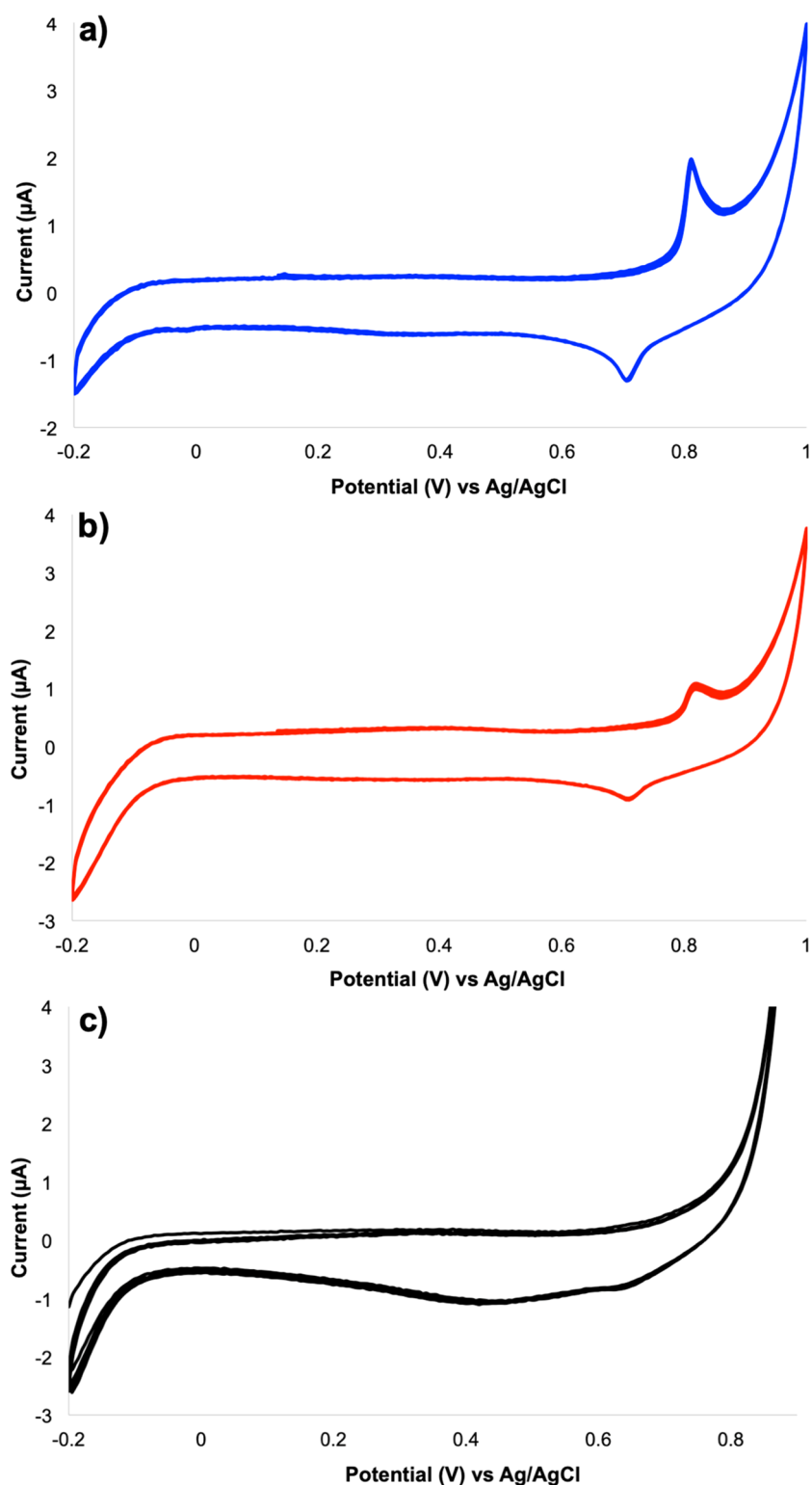
Figure 4. Cyclic voltammograms for 0.5 mM U^{IV}-343-HOPO complexes collected at a scan rate of 100 mV/s in (a) 1 M SO_4^{2-} at pH 2.3, (b) 1 M NO_3^- at pH 1.3, and (c) 1 M Cl^- at pH 1.3.

Note that the *r*-axis in Figure 3 differs from the actual bond lengths due to known phase shift effects and therefore fits to known, or calculated,[51] lineshapes are required to extract metrical information.

Qualitatively, the EXAFS signals are well described by a fitting model based on calculated tetravalent and hexavalent An-HOPO structures.[42,52] The fitting models for all three U^{IV}

complexes could not be satisfactorily fit as only U^{IV} species due to the substantial features near 1.4 Å in the FTs at low *r* that are unaccounted for in U^{IV}-only models (Figure 3). Such features are indicative of the axial U—O pairs (hereby denoted U—O_{ax}) of an "yl" complex[42] and are consistent with the presence of the high energy shoulder in the XANES spectra for each of the U^{IV}-343-chelator complexes (Figure 2). When fits
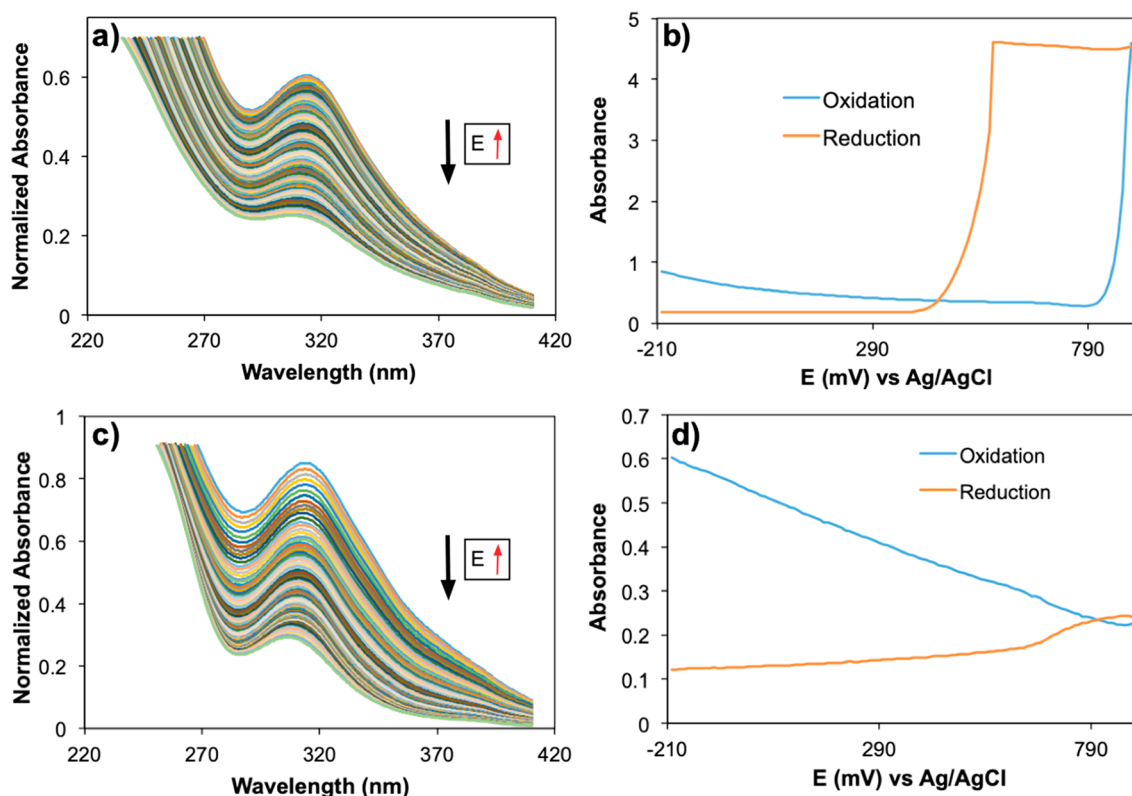
Figure 5. Normalized UV−vis absorption spectra between −200 and 750 mV versus Ag/AgCl of 0.5 mM [U^{IV}-343-HOPO] in (a) 1 M SO_4^{2-} at pH 2.3 and (c) 1 M Cl^- at pH 1.3, recorded with 30-s steps for each 10 mV. 343-HOPO maximum absorbance versus potential for (b) 1 M SO_4^{2-} at pH 2.3 and (d) 1 M Cl^- at pH 1.3. Wavelengths of maximum absorbance range from 307.5 to 313.5 nm for panels b and d. Path length: 1 cm. Absorbance corrected from blank background electrolyte for each sample. T = 25 °C.

to the EXAFS spectra for each complex are updated to account for a contribution from U−O_{ax} scatterers, fit statistics improve significantly. Focusing on the U^{IV}-343-HOPO complex, the fitting model attributes the first scattering shell to eight U−O scatterers, with a contribution from two U−O_{ax} scatterers (for the full model and results, see the Supporting Information). Using this model generates a high quality fit to the EXAFS data (Figure 3), and the fit results are broadly consistent with coordination to HOPO ligands. Beyond the short U−O_{ax} distances, U−O bond distances with 343-HOPO were found to be at an average of 2.39(1) Å, which is in excellent agreement with M^{IV}−O distances of 2.38 Å predicted by density functional theory calculations for U^{IV}.[52] A pair of U−O_{ax} scatterers at a bond length of approximately 1.75 Å (in contrast to ~2.4 Å for U−O scatterers in the equatorial plane) would be diagnostic of a pure U^{VI} sample. The fit for U^{IV}-343-HOPO yielded 0.7(3) U−O_{ax} scatterers at 1.74(2) Å implying approximately 35% U^{VI} in this sample. We observe similar results in the fit models of U^{IV}-343-HCCH and U^{IV}-343-CHHC (Figure 3), where U−O coordination to the 343-ligands (second shell) is attributed to eight U−O scatterers for both U^{IV}-343-HCCH and U^{IV}-343-CHHC, with an average U−O bond distance of 2.39(2) Å for both complexes. Similar to what was observed with 343-HOPO, there was also a contribution from U−O_{ax} scatterers indicative of the presence of U^{VI}. The fitting models for both U^{IV}-343-HCCH and U^{IV}-343-CHHC include 1.2(3) U−O_{ax} scatterers (equivalent to 60% U^{VI}) at approximately 1.76(1) and 1.78(1) Å, respectively. Collectively, along with XANES signatures, these EXAFS results indicate that each species is a

heterogeneous mixed valent U^{VI}/U^{IV} complex, similar to what we recently observed and reported for 343-HCCH with neptunium.[22]

The EXAFS spectrum of U^{VI}-343-HOPO has been collected previously[10] but was recollected here to allow for comparison with U^{IV}-343-HOPO, as well as U^{VI} complexes with the other 343-chelators. The FT of the EXAFS spectra for U^{VI} with all four 343-chelators revealed the characteristic two peaks that are well-known for actinyl moieties (Figure S2, Supporting Information). As a result, we included approximately two U−O_{ax} scatterers at values ranging from 1.75 to 1.79 Å in the first shell of the U^{VI}-343-ligand fits, and the second shell of the U^{VI}-343-chelator fits included six U−O scatterers at an average value of 2.42 Å (Table S2, Supporting Information). For all four U^{VI} complexes, U^{VI}−O bond distances in the axial and equatorial planes of the uranyl cation are found to be characteristic for uranyl species, which is consistent with previous experimental and theoretical reports on U^{VI}-343-HOPO.[10,52]

Electrochemical Measurements. To gain insight into the electrochemical stability of U^{IV} and U^{VI} complexes in aqueous media, CV and SEC measurements were carried out over the potential range of −200 mV to 1000 mV (vs Ag/AgCl electrode) at a sweep rate (v) of 100 mV/s. 343-HOPO was selected as the ligand of choice for all electrochemical measurements described herein, as it forms the most stable complexes with U^{IV} of any of the 343-chelators (*vide supra*), and the electrochemical behavior of the free chelator has been previously described.[17,22] Voltammograms of [U^{IV}-(343-HOPO)] complexes made *in situ* revealed a well-defined

reversible redox reaction directly after sample preparation when Na_2SO_4 and $NaNO_3$ were the background electrolyte, and this behavior was consistent across a range of sweep rates (Figure 4 and Table S3, Supporting Information). With NaCl as the background electrolyte, we note that results differ since in this system no redox events take place within the measurement window, which may be a result of high current masking the zone of interest (Figure 4). We attribute the reaction in sulfate and nitrate media to a U^{VI}/U^{IV} two-electron oxidation process, with the observed $E_{1/2}$ values of 756(7) mV versus Ag/AgCl using Na_2SO_4 and $E_{1/2}$ = 761(1) mV versus Ag/AgCl for $NaNO_3$ in excellent agreement with calculated values based on experimentally derived and predicted log β values for U^{IV}- and U^{VI}-343-HOPO.[17,23] Peak-to-peak separation $\Delta E = |E_{pa} - E_{pc}|$ is 106(12) mV for Na_2SO_4 and 102(7) mV for $NaNO_3$, with a sweep rate of 100 mV/s, indicating that these two systems may exhibit non-Nernstian responses. Such non-Nernstian behavior in these systems may be a result of an electrode absorbed event but may also be due to kinetics arising from an incompatible rate of ligand complexation with the rates of uranyl oxo activation and bond cleavage.[53]

The $\pi-\pi^*$ spectral band of 343-HOPO is at ~305 nm in acidic media, and is sensitive to metal binding (*vide supra*), which manifests as both changes in extinction coefficient as well as in the wavelength of max absorbance. More recently, a correlation between actinide oxidation state and the position of the 343-HOPO $\pi-\pi^*$ band was demonstrated for tetravalent metal cations,[19] and based on these findings, we anticipate the absorption band of 343-HOPO upon binding to U^{IV} should appear at ~310 nm. SEC measurements of [U^{IV}-343-HOPO] using sulfate as a background electrolyte resulted in a ligand-based band at 310(2) nm, indicative of the [U^{IV}-343-HOPO] complex rather than [U^{V}-343-HOPO]$^+$ or [U^{VI}-343-HOPO]$^{2+}$ species (Figure 5). Similarly, in chloride media, the ligand-based band was found to be at 310(3) nm, also indicative of the [U^{IV}-343-HOPO] complex (Figure 5). Notably, SEC characterization of U^{IV}-343-HOPO in 1 M Cl$^-$ features the same singularity that was observed using CV, specifically high current over the sweep range −200 to 1000 mV. This may be a result of a quick oxidation of the solvent, although it is possible a catalytic process is taking place. Such behavior for uranium has precedent, particularly in nonaqueous systems, as evidenced by the production of chlorine from HCl using uranium oxides,[54] although this was not something we investigated as part of this study. On the basis of the shape of both the raw results and the plots of maximum absorbance versus potential (Figure 5b,d), it appears that Cl$^-$ may also enhance the catalytic properties of uranium in this system with 343-HOPO, and this is an area of ongoing investigation in our lab.

After 48 h, the reversible redox reactions noted in Figure 4 were no longer observed in either sulfate or nitrate media, while the voltammogram using chloride as a background electrolyte remained stable over time (Figure S4, Supporting Information). We hypothesize that this change in electrochemical behavior is explained by the extraordinary stability of [U^{IV}-343-HOPO], which is also a thermodynamically favored product, as reoxidation to U^{V} or U^{VI} would involve the addition of one or two electron(s) and a modification of the coordination number to allow for the addition of two axial oxygen atoms. We also considered redox processes involving the reduction of U^{VI} to U^{V} and the subsequent disproportio-

nation of U^{V} as there is some precedent for this redox pathway;[26,29] however, U^{IV} after U^{V} disproportionation is often observed in the form of UO_2,[28] and we saw no evidence of this species spectroscopically.[55] Thus, the growing peaks on the reduction side in the SEC maximum absorbance versus potential plots (Figure 5b,d) are not due to uranium, rather they are likely a result of either a reduction of the amount of water oxidized during the oxidation offset or a reduction of gold from the working electrode due to an electrode absorbed event.

CONCLUSIONS

In summary, chelation and stabilization of U^{IV} were observed in condensed aqueous phases. With 343-HOPO, UV−visible spectrophotometry indicated formation of a U^{IV} complex that is practically inert toward oxidation or hydrolysis in acidic, aqueous solution. XANES and EXAFS spectroscopies on U^{IV}- and U^{VI}-343 ligand complexes confirmed metal ion binding, and provided some of the first structural data on heterogeneous mixed valent U^{VI}/U^{IV} chelates, at physiologically relevant pH. Additionally, these results indicate that 343-ligands can stabilize U^{IV} outside the acidic pH window, which is very unusual, and also aid in understanding previously observed U-343-HOPO decorporation results.[12] CV and SEC measurements demonstrated that the U^{IV} complex with 343-HOPO is relatively stable after approximately 48 h, and U^{VI} ions can be reduced in aqueous systems, likely proceeding via a two-electron reduction process similar to what has been observed recently in both aqueous and nonaqueous systems.[27,33] As An^{VI}/An^{IV} interactions are of significant importance in the nuclear reprocessing and actinide migration schemes, work is in progress to better understand the conditions over which different uranium species are stable in solution, which is important for the development of reliable models that accurately predict the chemical behavior of these radionuclides in chemical, biological, and environmental systems. Moreover, we aim to extend the chemistry highlighted herein to other actinyl systems including protactinium, plutonium, and americium.

ASSOCIATED CONTENT

Ⓢ **Supporting Information**

The Supporting Information is available free of charge at https://pubs.acs.org/doi/10.1021/acs.inorgchem.0c03088.

> Experimental details, additional UV−vis absorbance spectra, additional figures and tables from XANES and EXAFS spectra, additional electrochemistry spectra and parameters (PDF)

AUTHOR INFORMATION

Corresponding Authors

Rebecca J. Abergel − *Chemical Sciences Division, Lawrence Berkeley National Laboratory, Berkeley, California 94720, United States; Department of Nuclear Engineering, University of California, Berkeley, California 94709, United States;* Ⓞ orcid.org/0000-0002-3906-8761; Email: abergel@berkeley.edu

Corwin H. Booth − *Chemical Sciences Division, Lawrence Berkeley National Laboratory, Berkeley, California 94720, United States;* Ⓞ orcid.org/0000-0001-6827-0080; Email: chbooth@lbl.gov

Authors

Korey P. Carter − *Chemical Sciences Division, Lawrence Berkeley National Laboratory, Berkeley, California 94720, United States;* ◉ orcid.org/0000-0003-4191-0740

Kurt F. Smith − *Chemical Sciences Division, Lawrence Berkeley National Laboratory, Berkeley, California 94720, United States*

Toni Tratnjek − *Chemical Sciences Division, Lawrence Berkeley National Laboratory, Berkeley, California 94720, United States*

Gauthier J.-P. Deblonde − *Chemical Sciences Division, Lawrence Berkeley National Laboratory, Berkeley, California 94720, United States; Glenn T. Seaborg Institute, Physical & Life Sciences, Lawrence Livermore National Laboratory, Livermore, California 94550, United States;* ◉ orcid.org/0000-0002-0825-8714

Liane M. Moreau − *Chemical Sciences Division, Lawrence Berkeley National Laboratory, Berkeley, California 94720, United States;* ◉ orcid.org/0000-0003-4381-8753

Julian A. Rees − *Chemical Sciences Division, Lawrence Berkeley National Laboratory, Berkeley, California 94720, United States;* ◉ orcid.org/0000-0003-0883-2680

Complete contact information is available at:
https://pubs.acs.org/10.1021/acs.inorgchem.0c03088

Notes

The authors declare no competing financial interest.

■ REFERENCES

(1) Koch-Steindl, H.; Pröhl, G. Considerations on the behaviour of long-lived radionuclides in the soil. *Radiat. Environ. Biophys.* **2001**, *40* (2), 93−104.

(2) Newsome, L.; Morris, K.; Lloyd, J. R. The biogeochemistry and bioremediation of uranium and other priority radionuclides. *Chem. Geol.* **2014**, *363*, 164−184.

(3) Carter, K. P.; Surbella, R. G., III; Kalaj, M.; Cahill, C. L. Restricted Speciation and Supramolecular Assembly in the 5f Block. *Chem. - Eur. J.* **2018**, *24*, 12747−12756.

(4) Gorden, A. E. V.; Xu, J.; Raymond, K. N.; Durbin, P. Rational Design of Sequestering Agents for Plutonium and Other Actinides. *Chem. Rev.* **2003**, *103* (11), 4207−4282.

(5) Sockwell, A. K.; Wetzler, M. Beyond Biological Chelation: Coordination of f-Block Elements by Polyhydroxamate Ligands. *Chem. - Eur. J.* **2019**, *25* (10), 2380−2388.

(6) Surbella, III, R. G.; Cahill, C. L. Hybrid Materials of the f-Elements Part II: The Uranyl Cation. In *Handbook on the Physics and Chemistry of Rare Earths*; Bünzli, J.-C. G., Pecharsky, V. K., Eds.; Elsevier: Amsterdam, 2015; Vol. 48, pp 163−285.

(7) Lu, G.; Haes, A. J.; Forbes, T. Z. Detection and identification of solids, surfaces, and solutions of uranium using vibrational spectroscopy. *Coord. Chem. Rev.* **2018**, *374*, 314−344.

(8) Ansoborlo, E.; Prat, O.; Moisy, P.; Den Auwer, C.; Guilbaud, P.; Carriere, M.; Gouget, B.; Duffield, J.; Doizi, D.; Vercouter, T.; Moulin, C.; Moulin, V. Actinide speciation in relation to biological processes. *Biochimie* **2006**, *88* (11), 1605−1618.

(9) Vidaud, C.; Bourgeois, D.; Meyer, D. Bone as Target Organ for Metals: The Case of f-Elements. *Chem. Res. Toxicol.* **2012**, *25* (6), 1161−1175.

(10) Younes, A.; Creff, G.; Beccia, M. R.; Moisy, P.; Roques, J.; Aupiais, J.; Hennig, C.; Solari, P. L.; Den Auwer, C.; Vidaud, C. Is hydroxypyridonate 3,4,3-LI(1,2-HOPO) a good competitor of fetuin for uranyl metabolism? *Metallomics* **2019**, *11* (2), 496−507.

(11) Abergel, R. J.; Durbin, P. W.; Kullgren, B.; Ebbe, S. N.; Xu, J.; Chang, P. Y.; Bunin, D. I.; Blakely, E. A.; Bjornstad, K. A.; Rosen, C. J.; Shuh, D. K.; Raymond, K. N. Biomimetic Actinide Chelators: An Update on the Preclinical Development of the Orally Active Hydroxypyridonate Decorporation Agents 3,4,3-LI(1,2-HOPO) and 5-LIO(Me-3,2-HOPO). *Health Phys.* **2010**, *99* (3), 401−407.

(12) Kullgren, B.; Jarvis, E. E.; An, D. D.; Abergel, R. J. Actinide chelation: biodistribution and in vivo complex stability of the targeted metal ions. *Toxicol. Mech. Methods* **2013**, *23* (1), 18−26.

(13) Cilibrizzi, A.; Abbate, V.; Chen, Y.-L.; Ma, Y.; Zhou, T.; Hider, R. C. Hydroxypyridinone Journey into Metal Chelation. *Chem. Rev.* **2018**, *118* (16), 7657−7701.

(14) Ricano, A.; Captain, I.; Carter, K. P.; Nell, B. P.; Deblonde, G. J.-P.; Abergel, R. J. Combinatorial design of multimeric chelating peptoids for selective metal coordination. *Chemical Science* **2019**, *10* (28), 6834−6843.

(15) Durbin, P. W.; Kullgren, B.; Xu, J.; Raymond, K. N. Development of Decorporation Agents for the Actinides. *Radiat. Prot. Dosim.* **1998**, *79* (1−4), 433−443.

(16) Abergel, R. J. Chelation of Actinides. In *Metal Chelation in Medicine*; Crichton, R., Ward, R. J., Hider, R. C., Eds.; The Royal Society of Chemistry: Cambridge, UK, 2017; pp 183−212.

(17) Deblonde, G. J.-P.; Sturzbecher-Hoehne, M.; Abergel, R. J. Solution Thermodynamic Stability of Complexes Formed with the Octadentate Hydroxypyridinonate Ligand 3,4,3-LI(1,2-HOPO): A Critical Feature for Efficient Chelation of Lanthanide(IV) and Actinide(IV) Ions. *Inorg. Chem.* **2013**, *52* (15), 8805−8811.

(18) Sturzbecher-Hoehne, M.; Choi, T. A.; Abergel, R. J. Hydroxypyridinonate Complex Stability of Group (IV) Metals and Tetravalent f-Block Elements: The Key to the Next Generation of Chelating Agents for Radiopharmaceuticals. *Inorg. Chem.* **2015**, *54* (7), 3462−3468.

(19) Deblonde, G. J.-P.; Sturzbecher-Hoehne, M.; Rupert, P. B.; An, D. D.; Illy, M.-C.; Ralston, C. Y.; Brabec, J.; de Jong, W. A.; Strong, R. K.; Abergel, R. J. Chelation and stabilization of berkelium in oxidation state + IV. *Nat. Chem.* **2017**, *9*, 843−849.

(20) Deblonde, G. J.-P.; Lohrey, T. D.; An, D. D.; Abergel, R. J. Toxic heavy metal - Pb, Cd, Sn - complexation by the octadentate hydroxypyridinonate ligand archetype 3,4,3-LI(1,2-HOPO). *New J. Chem.* **2018**, *42* (10), 7649−7658.

(21) Deblonde, G. J.-P.; Lohrey, T. D.; Abergel, R. J. Inducing selectivity and chirality in group IV metal coordination with high-denticity hydroxypyridinones. *Dalton Transactions* **2019**, *48* (23), 8238−8247.

(22) Carter, K. P.; Smith, K. F.; Tratnjek, T.; Shield, K. M.; Moreau, L. M.; Rees, J. A.; Booth, C. H.; Abergel, R. J. Spontaneous Chelation-Driven Reduction of the Neptunyl Cation in Aqueous Solution. *Chem. - Eur. J.* **2020**, *26* (11), 2354−2359.

(23) Sturzbecher-Hoehne, M.; Deblonde, G. J.-P.; Abergel, R. J. Solution thermodynamic evaluation of hydroxypyridinonate chelators 3,4,3-LI(1,2-HOPO) and 5-LIO(Me-3,2-HOPO) for UO_2(VI) and Th(IV) decorporation. *Radiochim. Acta* **2013**, *101* (6), 359−366.

(24) Carter, K. P.; Jian, J.; Pyrch, M. M.; Forbes, T. Z.; Eaton, T. M.; Abergel, R. J.; de Jong, W. A.; Gibson, J. K. Reductive activation of neptunyl and plutonyl oxo species with a hydroxypyridinone chelating ligand. *Chem. Commun.* **2018**, *54* (76), 10698−10701.

(25) Cahill, C. L.; Burns, P. C. Building Unit and Topological Evolution in the Hydrothermal DABCO−U−F System. *Inorg. Chem.* **2001**, *40* (6), 1347−1351.

(26) Bell, N. L.; Shaw, B.; Arnold, P. L.; Love, J. B. Uranyl to Uranium(IV) Conversion through Manipulation of Axial and Equatorial Ligands. *J. Am. Chem. Soc.* **2018**, *140* (9), 3378−3384.

(27) Faizova, R.; Fadaei-Tirani, F.; Bernier-Latmani, R.; Mazzanti, M. Ligand-Supported Facile Conversion of Uranyl(VI) into Uranium-(IV) in Organic and Aqueous Media. *Angew. Chem., Int. Ed.* **2020**, *59* (17), 6756−6759.

(28) Kretzschmar, J.; Haubitz, T.; Hübner, R.; Weiss, S.; Husar, R.; Brendler, V.; Stumpf, T. Network-like arrangement of mixed-valence uranium oxide nanoparticles after glutathione-induced reduction of uranium(VI). *Chem. Commun.* **2018**, *54* (63), 8697−8700.

(29) Vettese, G. F.; Morris, K.; Natrajan, L. S.; Shaw, S.; Vitova, T.; Galanzew, J.; Jones, D. L.; Lloyd, J. R. Multiple Lines of Evidence Identify U(V) as a Key Intermediate during U(VI) Reduction by Shewanella oneidensis MR1. *Environ. Sci. Technol.* **2020**, *54* (4), 2268−2276.

(30) Dovrat, G.; Illy, M.-C.; Berthon, C.; Lerner, A.; Mintz, M. H.; Maimon, E.; Vainer, R.; Ben-Eliyahu, Y.; Moiseev, Y.; Moisy, P.; Bettelheim, A.; Zilbermann, I. On the Aqueous Chemistry of the U^{IV}−DOTA Complex. *Chem. - Eur. J.* **2020**, *26* (15), 3390−3403.

(31) Pedrick, E. A.; Wu, G.; Hayton, T. W. Oxo Ligand Substitution in a Cationic Uranyl Complex: Synergistic Interaction of an Electrophile and a Reductant. *Inorg. Chem.* **2015**, *54* (14), 7038−7044.

(32) Kiernicki, J. J.; Zeller, M.; Bart, S. C. Facile Reductive Silylation of UO_2^{2+} to Uranium(IV) Chloride. *Angew. Chem., Int. Ed.* **2017**, *56* (4), 1097−1100.

(33) Rice, N. T.; McCabe, K.; Bacsa, J.; Maron, L.; La Pierre, H. S. Two-Electron Oxidative Atom Transfer at a Homoleptic, Tetravalent Uranium Complex. *J. Am. Chem. Soc.* **2020**, *142* (16), 7368−7373.

(34) Captain, I.; Deblonde, G. J.-P.; Rupert, P. B.; An, D. D.; Illy, M.-C.; Rostan, E.; Ralston, C. Y.; Strong, R. K.; Abergel, R. J. Engineered Recognition of Tetravalent Zirconium and Thorium by Chelator−Protein Systems: Toward Flexible Radiotherapy and Imaging Platforms. *Inorg. Chem.* **2016**, *55* (22), 11930−11936.

(35) Knope, K. E.; Soderholm, L. Solution and Solid-State Structural Chemistry of Actinide Hydrates and Their Hydrolysis and Condensation Products. *Chem. Rev.* **2013**, *113* (2), 944−994.

(36) Jung, K.-S.; Sohn, S. C.; Ha, Y. K.; Eom, T. Y.; Yun, S. S. Electrochemical reduction mechanism of EDTA complexes of U^{4+} and UO^{2+}_2 at HMDE in aqueous solution. *J. Electroanal. Chem. Interfacial Electrochem.* **1991**, *315* (1), 113−124.

(37) Natrajan, L. S.; Swinburne, A. N.; Andrews, M. B.; Randall, S.; Heath, S. L. Redox and environmentally relevant aspects of actinide(IV) coordination chemistry. *Coord. Chem. Rev.* **2014**, *266−267*, 171−193.

(38) Wacker, J. N.; Vasiliu, M.; Huang, K.; Baumbach, R. E.; Bertke, J. A.; Dixon, D. A.; Knope, K. E. Uranium(IV) Chloride Complexes: UCl_6^{2-} and an Unprecedented $U(H_2O)_4Cl_4$ Structural Unit. *Inorg. Chem.* **2017**, *56* (16), 9772−9780.

(39) Kent, G. T.; Wu, G.; Hayton, T. W. Synthesis and Crystallographic Characterization of the Tetravalent Actinide-DOTA Complexes [$An^{IV}(\kappa^8$-DOTA)(DMSO)] (An = Th, U). *Inorg. Chem.* **2019**, *58* (13), 8253−8256.

(40) Vanagas, N. A.; Higgins, R. F.; Wacker, J. N.; Asuigui, D. R. C.; Warzecha, E.; Kozimor, S. A.; Stoll, S. L.; Schelter, E. J.; Bertke, J. A.; Knope, K. E. Mononuclear to Polynuclear U^{IV} Structural Units: Effects of Reaction Conditions on U-Furoate Phase Formation. *Chem. - Eur. J.* **2020**, *26* (26), 5872−5886.

(41) Deblonde, G. J.-P.; Ricano, A.; Abergel, R. J. Ultra-selective ligand-driven separation of strategic actinides. *Nat. Commun.* **2019**, *10* (1), 2438.

(42) Allen, P. G.; Bucher, J. J.; Shuh, D. K.; Edelstein, N. M.; Reich, T. Investigation of Aquo and Chloro Complexes of UO_2^{2+}, NpO_2^+, Np^{4+}, and Pu^{3+} by X-ray Absorption Fine Structure Spectroscopy. *Inorg. Chem.* **1997**, *36* (21), 4676−4683.

(43) Loiseau, T.; Mihalcea, I.; Henry, N.; Volkringer, C. The crystal chemistry of uranium carboxylates. *Coord. Chem. Rev.* **2014**, *266−267* (0), 69−109.

(44) Martin, N. P.; März, J.; Volkringer, C.; Henry, N.; Hennig, C.; Ikeda-Ohno, A.; Loiseau, T. Synthesis of Coordination Polymers of Tetravalent Actinides (Uranium and Neptunium) with a Phthalate or Mellitate Ligand in an Aqueous Medium. *Inorg. Chem.* **2017**, *56* (5), 2902−2913.

(45) Wacker, J. N.; Han, S. Y.; Murray, A. V.; Vanagas, N. A.; Bertke, J. A.; Sperling, J. M.; Surbella, R. G.; Knope, K. E. From Thorium to Plutonium: Trends in Actinide(IV) Chloride Structural Chemistry. *Inorg. Chem.* **2019**, *58* (16), 10578−10591.

(46) Colliard, I.; Morrison, G.; Loye, H.-C. z.; Nyman, M. Supramolecular Assembly of U(IV) Clusters and Superatoms with Unconventional Countercations. *J. Am. Chem. Soc.* **2020**, *142* (19), 9039−9047.

(47) Moll, H.; Denecke, M. A.; Jalilehvand, F.; Sandström, M.; Grenthe, I. Structure of the Aqua Ions and Fluoride Complexes of Uranium(IV) and Thorium(IV) in Aqueous Solution an EXAFS Study. *Inorg. Chem.* **1999**, *38* (8), 1795−1799.

(48) Hennig, C.; Tutschku, J.; Rossberg, A.; Bernhard, G.; Scheinost, A. C. Comparative EXAFS Investigation of Uranium(VI) and -(IV) Aquo Chloro Complexes in Solution Using a Newly Developed Spectroelectrochemical Cell. *Inorg. Chem.* **2005**, *44* (19), 6655−6661.

(49) Hennig, C.; Schmeide, K.; Brendler, V.; Moll, H.; Tsushima, S.; Scheinost, A. C. EXAFS Investigation of U(VI), U(IV), and Th(IV) Sulfato Complexes in Aqueous Solution. *Inorg. Chem.* **2007**, *46* (15), 5882−5892.

(50) Ikeda-Ohno, A.; Hennig, C.; Tsushima, S.; Scheinost, A. C.; Bernhard, G.; Yaita, T. Speciation and Structural Study of U(IV) and -(VI) in Perchloric and Nitric Acid Solutions. *Inorg. Chem.* **2009**, *48* (15), 7201−7210.

(51) Ankudinov, A. L.; Ravel, B.; Rehr, J. J.; Conradson, S. D. Real-space multiple-scattering calculation and interpretation of X-ray-absorption near-edge structure. *Phys. Rev. B: Condens. Matter Mater. Phys.* **1998**, *58* (12), 7565−7576.

(52) Kelley, M. P.; Deblonde, G. J.-P.; Su, J.; Booth, C. H.; Abergel, R. J.; Batista, E. R.; Yang, P. Bond Covalency and Oxidation State of Actinide Ions Complexed with Therapeutic Chelating Agent 3,4,3-LI(1,2-HOPO). *Inorg. Chem.* **2018**, *57* (9), 5352−5363.

(53) Abergel, R. J.; de Jong, W. A.; Deblonde, G. J.-P.; Dau, P. D.; Captain, I.; Eaton, T. M.; Jian, J.; van Stipdonk, M. J.; Martens, J.; Berden, G.; Oomens, J.; Gibson, J. K. Cleaving Off Uranyl Oxygens through Chelation: A Mechanistic Study in the Gas Phase. *Inorg. Chem.* **2017**, *56* (21), 12930−12937.

(54) Amrute, A. P.; Krumeich, F.; Mondelli, C.; Pérez-Ramírez, J. Depleted uranium catalysts for chlorine production. *Chemical Science* **2013**, *4* (5), 2209−2217.

(55) Moreau, L. M.; Herve, A.; Straub, M. D.; Russo, D. R.; Abergel, R. J.; Alayoglu, S.; Arnold, J.; Braun, A.; Deblonde, G. J.-P.; Liu, Y.; Lohrey, T. D.; Olive, D. T.; Qiao, Y.; Rees, J. A.; Shuh, D. K.; Teat, S. J.; Booth, C. H.; Minasian, S. G. Structural properties of ultra-small thorium and uranium dioxide nanoparticles embedded in a covalent organic framework. *Chemical Science* **2020**, *11* (18), 4648−4668.